Electronic Supplementary Material (ESI) for Analyst.

Orientational binding modes of reporters in a viral-nanoparticle lateral-flow assay

Jinsu Kim,[a] Ryan Poling-Skutvik,[a] João R. C. Trabuco,[a] Katerina Kourentzi,[a] Richard C. Willson,[abc] and Jacinta C. Conrad*[a]

[a]Department of Chemical & Biomolecular Engineering, University of Houston, Houston, TX 77204, United States
[b]Department of Biology & Biochemistry, University of Houston, Houston, Texas 77004, United States
[c]Centro de Biotecnología FEMSA, Tecnológico de Monterrey, Monterrey, Nuevo León, Mexico

*Corresponding author: jcconrad@uh.edu

Movie S1. Biotinylated Fluor-M13 are imaged in capillary-driven transport through an LFA membrane that is functionalized with anti-M13 antibodies. The movie begins with liquid breakthrough in the field of view (208.3 μm × 213 μm); the frame rate is 30 frames/sec. Only the first 2000 frames after breakthrough are shown. Although the Reynolds number is low ($Re \ll 1$) on all time scales, the complex fiber geometry distorts the flow streamlines; here phage readily flow around the fibers and change direction on the pore scale.

Comparison of the degree of biotinylation of Biotinylated Fluor-M13 phage using an enzyme-linked immunosorbent assay (ELISA). AviTag-M13 phage display a peptide on the p3 tail protein, which can serve as a substrate for *Escherichia coli* biotin ligase and is inherently biotinylated at greater than 50% efficiency when grown in an *E. coli* host that contains the pBirA plasmid.[1] We complete the biotinylation *in vitro* using *E. coli* biotin ligase (birA) according to the manufacturer's instructions (Avidity AviTag Technology). The degrees of biotinylation of AviTag-M13 and Biotinylated Fluor-M13 are compared using TMB (3,3',5,5'-Tetramethylbenzidine)-ELISA. 100 μL of AviTag-M13 or 100 μL of Biotinylated Fluor-M13 at concentrations of 0, 10^4, 10^5, 10^6, 10^7, 10^8 and 10^9 pfu/mL in 2% (w/v) BSA are added to neutravidin-coated 96-well plates (Pierce Reacti-bind 96-well plates, Thermo Scientific #15128). After a 2 h incubation at room temperature, the plate is washed and rinsed four times each with PBST (PBS containing 0.05% (v/v) Tween 20) and PBS, respectively. Next, bound AviTag-M13 or Biotinylated Fluor-M13 are allowed to react with 100 μL of horseradish peroxidase (HRP)-

conjugated anti-M13 antibody (1:5,000 dilution) for 1 h at room temperature, followed by washing and rinsing. 50 μL of TMB (3,3′,5,5′- Tetramethylbenzidine) is added to the plate to develop the color for 15 min, and the reaction is terminated by adding 50 μL of 2 N H_2SO_4. Absorbance is measured at 450 nm in an ELISA reader (Tecan, Infinite M200 PRO). As the control experiments, we perform an ELISA test for wild type M13 (ATCC, #37468) and biotinylated Fluor-M13 on neutravidin- and BSA-coated 96-well microplates, respectively.

Both the AviTag-M13, which are inherently biotinylated by our *E. coli* host cells, and the *in vitro* biotinylated Fluor-M13 phage exhibit positive ELISA outputs (Figure S1). The *in vitro* biotinylated Fluor-M13 show 130% greater biotinylation compared to AviTag-M13. The wild type and biotinylated Fluor-M13 do not give ELISA signals on the neutravidin- and BSA-coated plates, respectively, confirming that the biotinylated Fluor-M13 are specifically bound to neutravidin-coated plates.

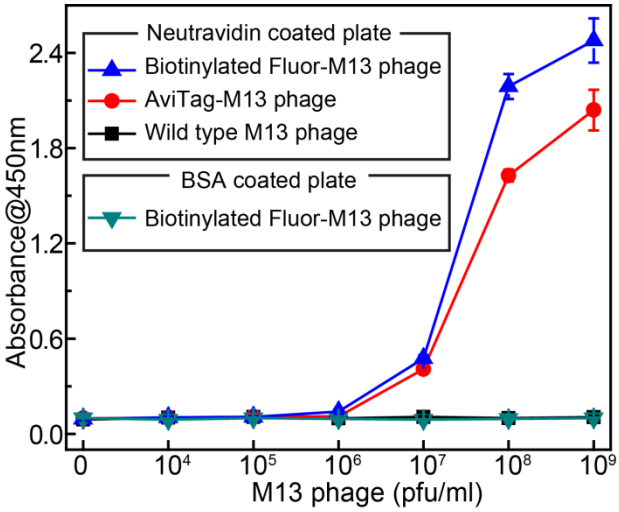

Figure S1. *Comparison of the degree of biotinylation.* Absorbance at a wavelength of 450 nm as a function of the concentration of M13 phage (TMB-ELISA). The AviTag-M13 exhibit positive TMB-ELISA outputs, confirming that they are inherently biotinylated by the *E. coli* host cells as expected. The *in vitro* biotinylated Fluor-M13 show 130% greater ELISA signal compared to AviTag-M13. The wild type and biotinylated Fluor-M13 do not give ELISA signals on the neutravidin- and BSA-coated plates, respectively, confirming that the biotinylated Fluor-M13 are specifically bound to neutravidin-coated plates.

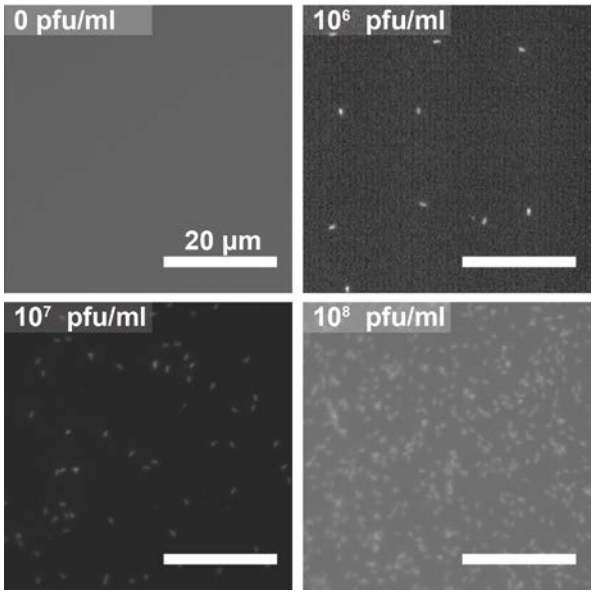

Figure S2. *Representative fluorescence micrographs of biotinylated Fluor-M13.* 10 µL of biotinylated Fluor-M13 at concentrations of 0, 10^6, 10^7 and 10^8 pfu/mL in PBS is dropped on coverslips and subsequently imaged using an epifluorescence microscope with 0.1 sec exposure time. The image contrast in each image is enhanced by histogram equalization. M13 phage are large enough to be imaged using optical microscopy as diffraction-limited objects when labeled with fluorescent dyes, and can be individually resolved.

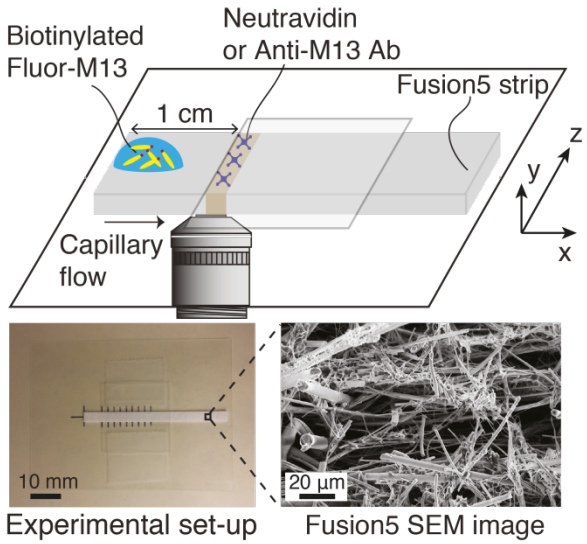

Figure S3. *Schematic of the experimental setup.* Fusion 5 glass membrane strips are modified with NeutrAvidin or with anti-M13 antibodies at a fixed distance of 1 cm from the distal end of the strip. Biotinylated-FluorM13 are dropped at the distal end of the Fusion 5 strip (representative scanning electron micrograph shown) and transported through capillary action along its length. Biotinylated Fluor-M13 are observed during flow using an epi-fluorescence microscope and imaged in real time at 30 frames/sec.

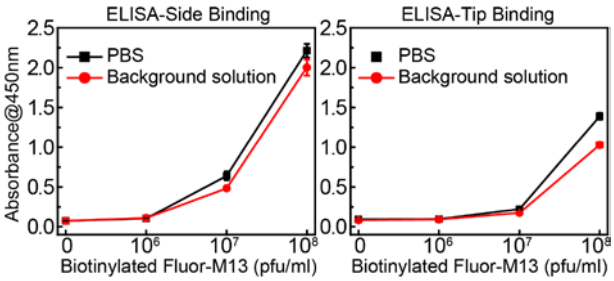

Figure S4. *Degree of binding for biotinylated Fluor-M13 in presence of the glycerol and the partially-hydrolyzed poly(acrylamide) (HPAM)*. TMB-ELISA is performed to determine if the background solution used in the flow-imaging experiments (30 v/v % glycerol and 0.2 w/v % HPAM in PBS) affects the binding interaction between biotinylated Fluor-M13 and anti-M13 antibody or neutravidin. Here, the degree of binding for phage in flow solution is compared to that in PBS buffer. For side-binding, we add biotinylated Fluor-M13 at concentrations of 0, 10^6, 10^7 and 10^8 pfu/mL in the background solution or PBS to a 96-well microplate that is coated with anti-M13 antibody. For tip-binding, biotinylated Fluor-M13 are added to a neutravidin-coated plate. After washing the plates, we add (HRP)-conjugated anti-M13 antibody to both plates, followed by washing and rinsing. After adding TMB to the plates, we measure the absorbance at 450 nm. The side- and tip-binding of the biotinylated Fluor-M13 are not significantly affected by the background solution; the difference in absorbance between binding in flow solution and in PBS buffer is less than 10%.

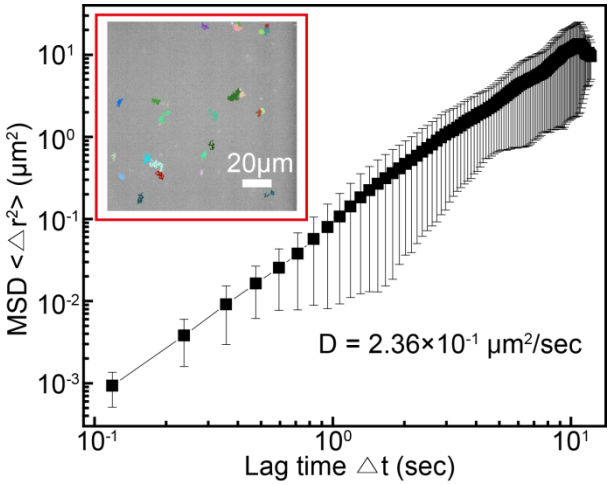

Figure S5. *Diffusivity of biotinylated Fluor-M13 in Fusion 5 membrane*. Two-dimensional ensemble-averaged mean-squared displacement (MSD) as a function of lag time Δt for biotinylated Fluor-M13 in a quiescent background solution (30 v/v % glycerol and 0.2 w/v % HPAM in PBS). The Fusion 5 membrane is filled with 10^7 pfu/ml phage sample, covered with a coverslip, and sealed with ultraviolet-curing epoxy. Phage undergoing Brownian diffusion are tracked using the particle tracking algorithm. The translational diffusion coefficient (D_p =2.36 × 10^{-1} μm^2/sec) is calculated from the slope of the linear relationship between MSD and lag time, i.e. $\langle \Delta r^2(\Delta t) \rangle = 4D_p \Delta t$.

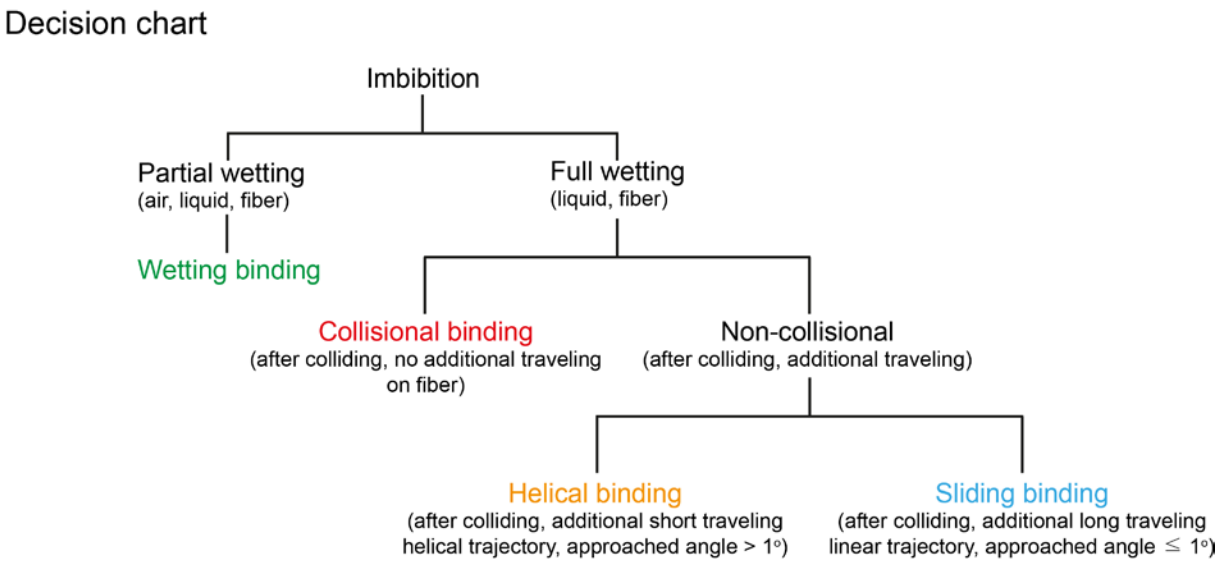

Figure S6. *Decision chart for classifying orientational binding modes.*

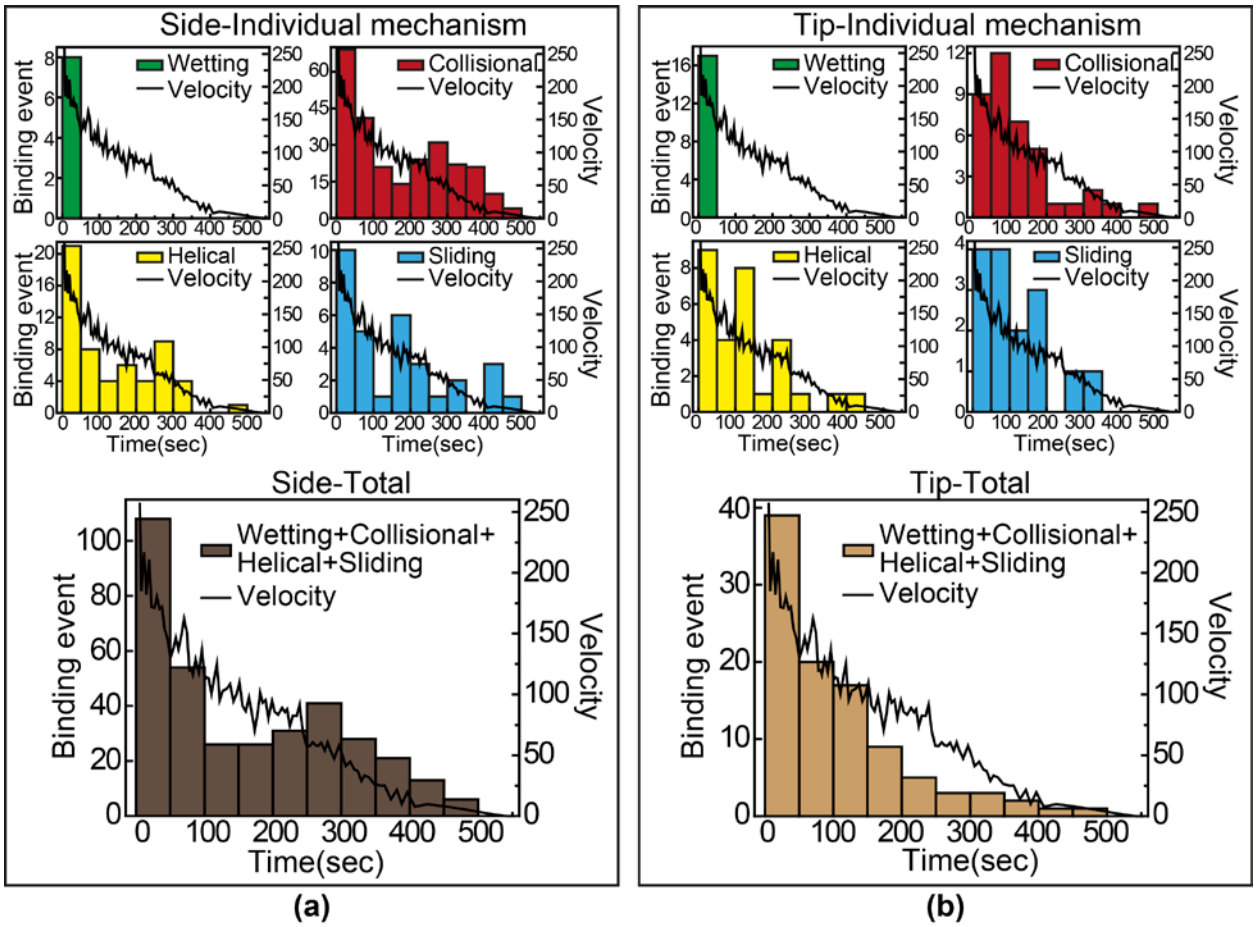

Figure S7. *Comparison of the binding time distributions and the local maximum velocity*. The binding time distribution and local maximum velocity are correlated. Both the number of (a) side- or (b) tip-binding phage and the local maximum velocity decrease as a function of time.

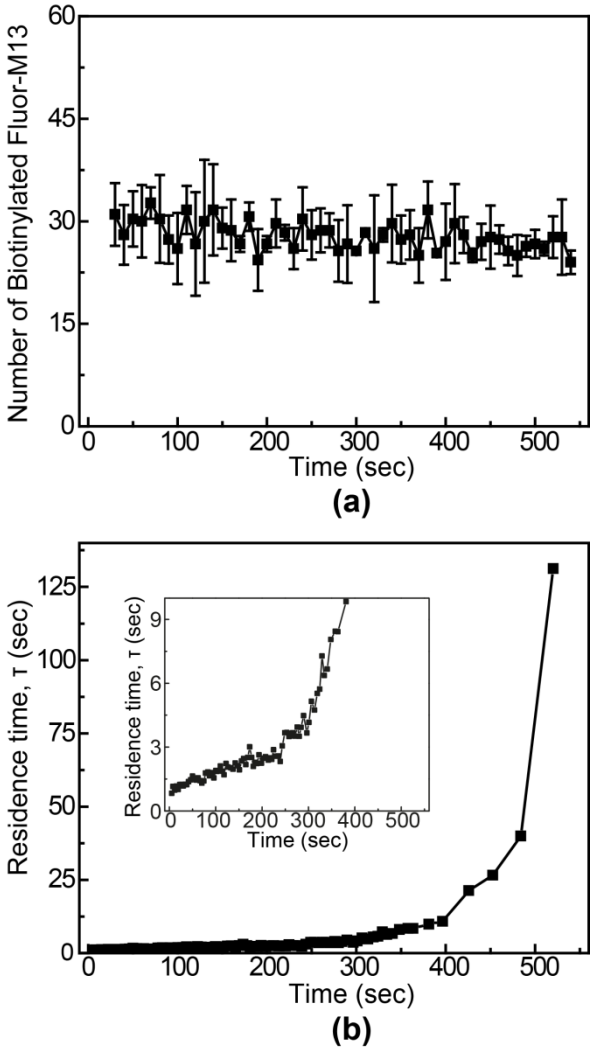

Figure S8. (a) Number of unbound phage in the field of view (208.3 μm × 213 μm) as a function of time. The number of unbound phage, 28 ± 2, was time-independent; the open pore network does not preclude phage transport. (b) Residence time of phage in the field of view. The residence time is calculated by multiplying 208.3 μm by $V(t)^{-1}$, where V(t) is the local maximum velocity. The residence time increases with the time after breakthrough (i.e. later-arriving phage have longer residence times).

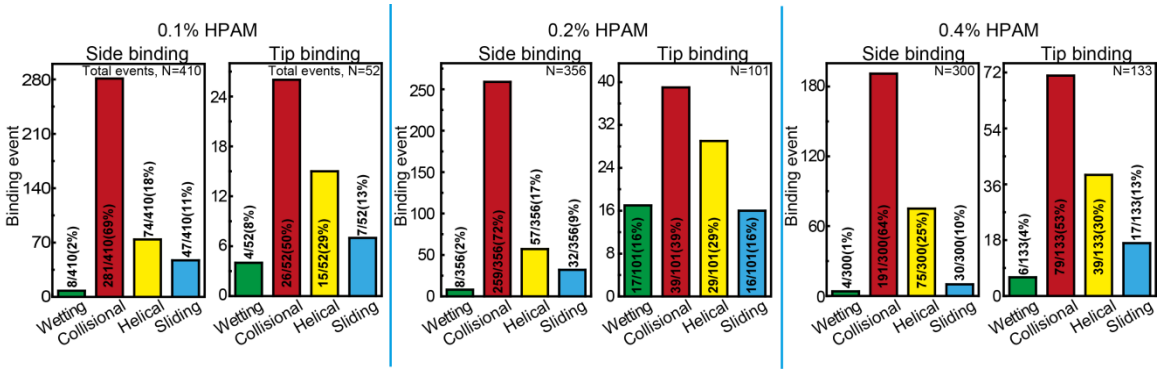

Figure S9. Comparison of orientational modes for side-binding and tip-binding in solutions of varying HPAM concentration (different fluid viscosities).

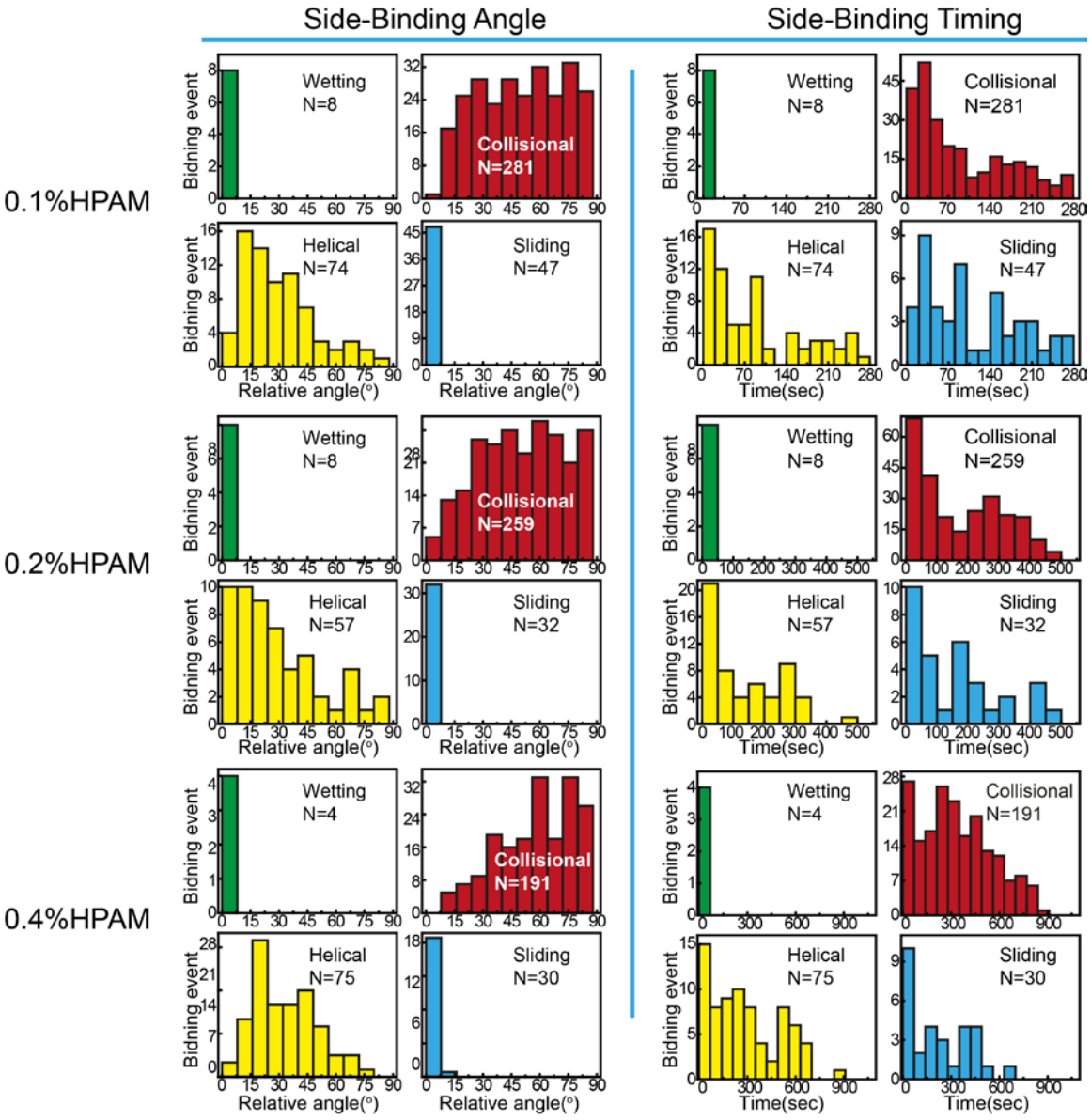

Figure S10. Relative angle and time for side-binding in solutions of various HPAM concentration (different fluid viscosities).

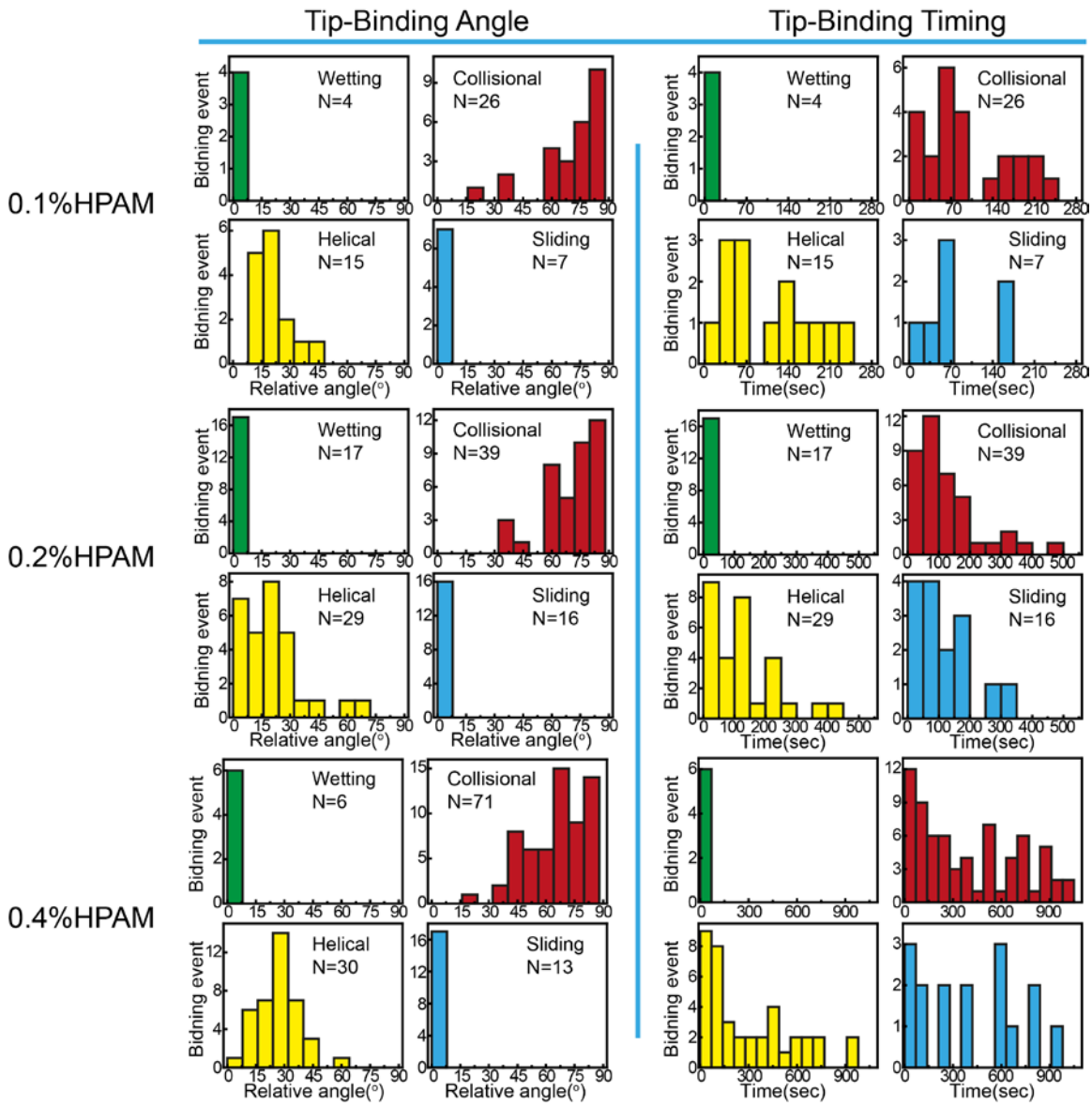

Figure S11. Relative angle and time for tip-binding for various concentrations of HPAM (different fluid viscosities).

References

(1) Scholle, M. D.; Kriplani, U.; Pabon, A.; Sishtla, K.; Glucksman, M. J.; Kay, B. K. Mapping Protease Substrates by Using a Biotinylated Phage Substrate Library. *Chembiochem* 2006, **7**, 834−838.